**AN IMPACT MODEL FOR THE ORIGIN OF ROCKY SURFACES AND MELT DEPOSITS AT THE ANTIPODE OF TYCHO CRATER.** I. S. Curren[1], D. A. Paige[1], and L. Esturas[1] [1]University of California Los Angeles, 595 Charles Young Drive East, Los Angeles, CA 90095-1567, iscurren@epss.ucla.edu.

**Introduction:** In a lunar far side region otherwise characterized as relatively old and heavily cratered highlands terrain, Lunar Reconnaissance Orbiter (LRO) thermal infrared, radar, and high-resolution imaging instruments have been used to identify a 7700 $km^2$ area centered around 42.5ºN, 167.5ºE that contains both rocky and smooth deposits typical of fresh impacts [1-5]. Diviner thermal observations reveal unusually high rock abundances and LROC high-resolution images reveal additional smooth deposits that appear to have been previously molten and resemble impact melt elsewhere on the lunar surface [1-5].

Ballistically emplaced impact ejecta has been postulated as the most likely source for the deposits, however crater size-frequency distributions in the region suggest an age that does not correspond to any proximal craters [1, 2]. Tycho crater provides the best fit for the estimated age (26 Ma) and volume (8 $km^3$) of the deposits [2]. Furthermore, ballistic modeling of the oblique Tycho impact has shown that ejecta would fall nearly antipode to Tycho crater, conisistent with the location of the deposits [6].

In this work we evaluate the Tycho ejecta emplacement hypothesis by examining the distribution of rocky and smooth units in the Tycho antipode region using LROC Narrow Angle Camera (NAC) images, Selene digital-elevation models (DEMs), and Diviner rock abundance data. We then present a one-dimensional energy balance model to explain the distribution and morphologies of the deposits assuming they are a product of Tycho impact ejecta.

**Observations:** The Tycho antipode region has a landscape typical of highlands terrain that has been blanketed by an atypical widespread but discontinuous layer of material. High-resolution images have revealed three distinct morphological units: (1) smooth ponded deposits, (2) widespread veneer deposits, and (3) rubble deposits that correspond to the high rock abundance values in the region [1-4, 7]. At the regional scale, veneer is widespread occurring as a <1 m-thick crust in intercrater plains [2] and as thicker deposits only within craters. Smooth ponds are observed within craters and depressions within intercrater plains, and rubble coincides primarily with crater walls and rims.

Using Global Mapper™ GIS software we have draped NAC images over Selene DEMs to perform local (crater-scale) mapping of the three morphological units in the area (Fig. 1). Focusing on lateral and slope distributions we find that: (1) ponds generally occur in the bottom of craters where slopes are a few degrees or less, (2) thick veneer deposits reminiscient of high-viscosity flows on Earth occur adjacent to ponds on slopes steeper than a few degrees but shallower than 45º, and (3) rubble terrain tends to occur upslope of veneer but does not occur at all azimuths.

Regional-scale observations illustrate that locations with the highest Diviner-derived rock abundance correspond with high slopes [7]. Crossplotting the two datasets confirms this positive correlation at the crater scale (Fig. 2). A a note, some high-rock abundance areas do occur on intermediate slopes within craters [4], but are associated with “fences”. These appear to be cracks in thick veneer at convex breaks in slope [2], which we consider secondary features that formed after the initial emplacement of ejecta from Tycho.

**Thermal Model:** Using a 1-dimensional energy

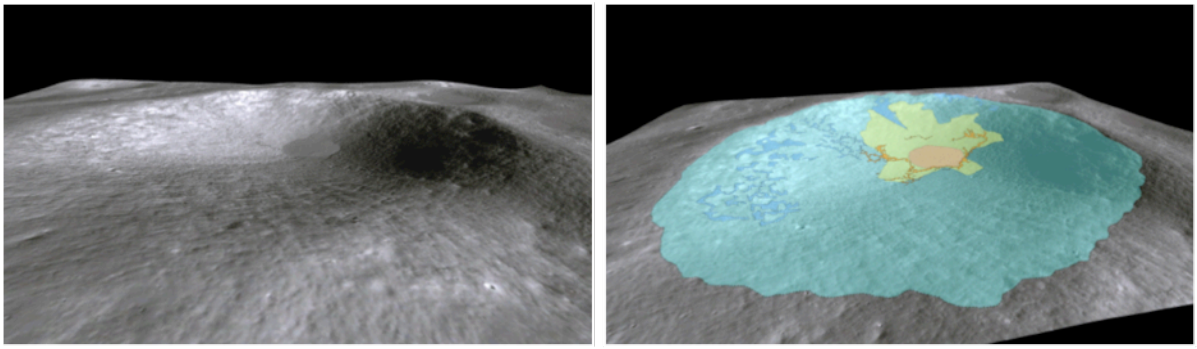

**Figure 1.** Oblique view of a crater centered at 43.32ºN, 167.34ºE within the Tycho antipode region. Light blue is rubble terrain, with darker blue indicating higher density rubble. Yellow represents thick veneer units, and light orange is ponded material. Sinuous orange deposits are rock fences occurring within veneer units. The NAC image, which is draped over a Selene DEM is 1.25x vertically exaggerated. The crater is ~ 20 km across along its widest axis.

balance model, we calculate the likelihood of melting from initially cold (i.e. not molten [8]) ejecta accumulation in the Tycho antipode region. Accumulation periods set for the model are derived from ballistic time of flight calculations for multiple Tycho antipodal trajectories, which indicate arrival times of < 2 hrs [6]. Half the kinetic energy associated with the ejecta impact velocity (~2.5 $kms^{-1}$) is assumed to result in heating, which is then balanced by infrared radiation to space, sensible heat storage in the ejecta, latent heat storage and release during melting, and thermal conduction into the subsurface.

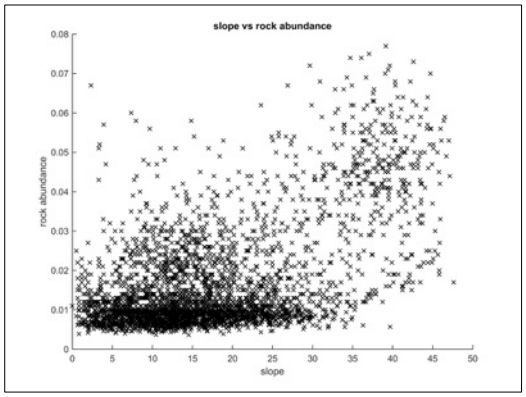


**Figure 2.** Diviner rock abundance data plotted against slope angle for the crater in Fig. 1.

The model shows a rapid rise in temperature during the ejecta accumulation period (blue box in Fig. 3), followed by a gradual cool down. Deposits are capable of plastic flow once they reach the liquidus of lunar highlands anorthosite. If ejecta accumulates rapidly (0.5 hrs), then 1-m and 0.5-m accruals are capable of plastic flow after 0.1255 and 0.29224 hours, respectively. Accumulations of less than 0.5 m does not yield melting in 0.5 hrs, implying that only relatively thick antipodal ejecta deposits will flow.

**Discussion:** Examination of the Tycho antipode reveals three distinct morphological units heterogenously distributed at both regional and local scales. At the crater scale, units exhibit slope dependence with ponds occuring on the lowest slopes, thick veneer on intermediate slopes, and rubble with high rock abundance on the steepest slopes. Rubble does not occur on all steep slopes meaning that ejecta is azimuthally anisotropic, which is consistent with other findings [4] and the oblique nature of the Tycho impact [9].

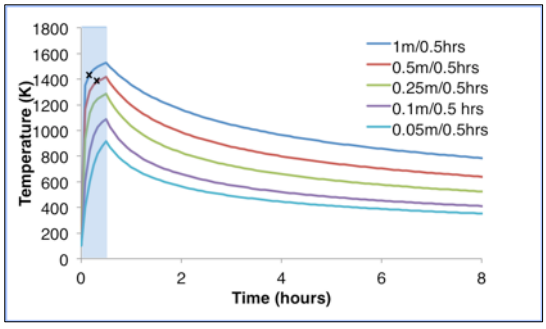


**Figure 3.** 1-D ejecta accumulation energy balance model. At t=0, deposits accumulate at a constant rate for 0.5 hrs. Point at which plastic deformation occurs is marked by x's.

Our thermal model implies that areas with conditions favorable for ejecta accumulation will reach temperatures high enough to cause melt and transient flow. Viscosites of melt are comparable to basaltic lavas on Earth [11-13], which is consistent with the lobed morphology of thick veneers. Accumulation in low-slope depressions would prevent downslope flow resulting in higher temperatures, lower viscosities, and subsequent viscous relaxation of the material, which is consistent with observed equipotential pond surfaces. Furthermore, pond size is independent of crater size, suggesting that ponds formed in place and are not the result of accumulation and downslope flow. We suspect that ejecta with incidence angles orthogonal to crater slopes would lose additional kinetic energy to work, resulting in the excavation of material and formation of rubble terrain. Areas that accumulate thin layers of antipodal ejecta, either due to unfavorable slopes, topographic shadowing, or distance from the antipode convergence point, are not predicted to undergo transient melting and flow and correspond to ejecta deposits that are found ubiquitously on the surface of the Moon.

Although the fast accumulation of ejecta from Tycho [6] suggests that multiple modes of emplacement were ongoing simultaneously (most likely a consequence of the ejecta incidence and crater slope intercept angle) we cannot yet rule out if the area underwent very fast multi-stage emplacement of ejecta [10]. Observations and modeling, however, are consistent with a highly distal ejecta emplacement model for the formation of rocky and surfaces and melt deposits at the antipode of Tycho crater.

**References:** [1] Robinson M.S. et al. (2011) *LPSC XLII,* 2511. [2] Robinson M.S. et al. (2015) *Icarus*, in press. [3] Bandfield J.L. et al. (2013) *LPSC XLIV*, 1770. [4] Bandfield J.L. et al. (2015) *Icarus,* in press. [5] Carter L.M. et al. (2012) *JGR*, *117*, E12. [6] Jögi P. and Paige D.A. (2014) *LPSC XLV*, 2574. [7] Curren I.S. et al. (2015) *AGU Fall Mtg.*, P53B-2111. [8] Artimieva N. (2013) *LPSC XLIV,* 1413. [9] Schultz P.H. and Anderson R.R. (1996) *Geol. Soc. Amer. Spec. Paper*, *302*, 397-417. [10] Osinski G.R. and Grieve R.A.F. (2011) *Earth and Planet. Sci. Lett.*, *310*, 167-181. [11] Handwerker C.A. et al. (1978) *Pergamom Press*, 483-493. [12] Murase T. and McBirney A.R. (1970) *Science, 167*, 1491-1493. [13] Råheim A. and Green D.H. (1974) *Journal Geol., 82,* 607-622.